

# Measurements of liquid film flow as a function of fluid properties and channel width: Evidence for surface-tension-induced long-range transverse coherence

A. Georgantaki,<sup>1,\*</sup> J. Vatteville,<sup>1,†</sup> M. Vlachogiannis,<sup>1,2,‡</sup> and V. Bontozoglou<sup>1,§</sup>

<sup>1</sup>*Department of Mechanical Engineering, University of Thessaly, GR-38334 Volos, Greece*

<sup>2</sup>*Technological Educational Institute of Larissa, GR-41110 Larissa, Greece*

(Received 17 January 2011; revised manuscript received 27 April 2011; published 24 August 2011)

We study experimentally the influence of the transverse dimension on film flow in relatively wide channels with sidewalls. Large deviations from two-dimensional predictions are observed in the primary instability and in the post-threshold traveling waves, and the deviations are presently shown to depend strongly on fluid physical properties. Measurements for a wide range of fluid properties are found to correlate with the Kapitza number, which represents the ratio of capillary to viscous stresses. These observations point to an unexpected long-range effect of surface tension that provides transverse coherence to the flow.

DOI: [10.1103/PhysRevE.84.026325](https://doi.org/10.1103/PhysRevE.84.026325)

PACS number(s): 47.15.gm, 47.35.Bb

## I. INTRODUCTION

Gravity-driven liquid films represent a good prototype of convectively unstable, open-flow systems, whose unstable band of wavelengths extends to zero [1–3]. This low-Reynolds-number interfacial system involves a complex balance between energy input, dissipation, dispersion, and nonlinearity that leads to the formation of pulselike coherent structures (solitary waves or dissipative solitons [4]), with each pulse containing a large number of phase-locked Fourier harmonics [5,6]. A key ingredient of this procedure, which differentiates the above coherent structures from classical solitons, is the cross-stream coherence to the flow provided by liquid viscosity [7].

The evolution of the flow from a base state with undisturbed interface is envisioned to occur through a Hopf bifurcation that involves strictly two-dimensional (2D) dynamics [8,9], according to Squire's theorem that proves the prevalence of disturbances in the streamwise direction. Subsequent spatiotemporal growth is considered to depend on the amount of noise in the transverse direction: with weak 3D noise content, the 2D flow development is taken to conclusion toward stationary solitary waves, whose crestlines may exhibit transverse modulations further downstream. With strong 3D noise, the first 2D stage may be infected by transverse modulations before concluding the streamwise evolution toward a solitary wave train [7,10–13]. The selection process of the transverse lengthscale of these modulations has been discussed in the above literature, and is typically much shorter than the width of the flow.

The aforementioned conceptual image is not fully supported by experimental realizations [14–16], and some specific issues have been questioned recently [17,18]. In particular, the latter investigations provide phenomenological evidence that the width of the flow has a puzzling and strong effect on both the onset of the primary instability and on the characteristics of stationary waves in the post-threshold regime. The present work attempts to uncover the prevailing physical mechanism

responsible for this behavior by performing and interpreting experiments with liquids of widely varying physical properties.

A first indication of unexpected behavior comes from experiments in flat channels bounded by sidewalls. Traveling disturbances beyond the primary threshold do not retain a straight crestline but become symmetrically curved around the centerplane. This wave characteristic can only be attributed to an effect of the sidewalls that evidently extends throughout the width of the channel. Symmetrically curved waves were shown to represent a very strong attractor of the flow at small channel inclinations [18]. As will be shown later, strong crestline curvature is related to the prevalence of capillary over viscous forces. Thus, it appears that surface tension determines characteristics of the flow over a distance that is orders of magnitude larger than the capillary length, i.e., it provides long-range transverse coherence.

Further evidence for an unexpected behavior of film flow comes from the observation [17] that the critical Reynolds number for the primary instability depends strongly on channel width. Significant deviations from the well-known prediction for 2D film flow at inclination  $\theta$  [19],  $Re_c^\circ = 5/6 \cot \theta$  (derived for unidirectional base flow and long, streamwise disturbances) were reported [17] for liquid films that extend in the transverse direction more than two orders of magnitude of the film thickness. Given that the base flow with a flat interface is known under these conditions to be one dimensional throughout the channel, with the exception of thin regions close to the sidewalls [20], Squire's theorem should apply. In spite of this, the instability appears to be strongly affected by side effects, and the two-dimensional evolution stage is completely bypassed.

## II. RESULTS

In order to understand the above phenomena, experiments were performed in two inclined flow facilities of adjustable width, with one 800 mm long by 250 mm wide and the other 3000 mm long by 450 mm wide. Inclination angles in the range  $\theta = 2\text{--}15^\circ$  were tested. The liquids used were aqueous solutions of glycerol or isopropanol. Data were parameterized in terms of two dimensionless numbers: (i) the Reynolds number  $Re$ , defined as the ratio of flow rate per unit span

\*ageorgan@uth.gr

†jvatteville@uth.gr

‡mvlach@teilar.gr

§bont@uth.gr

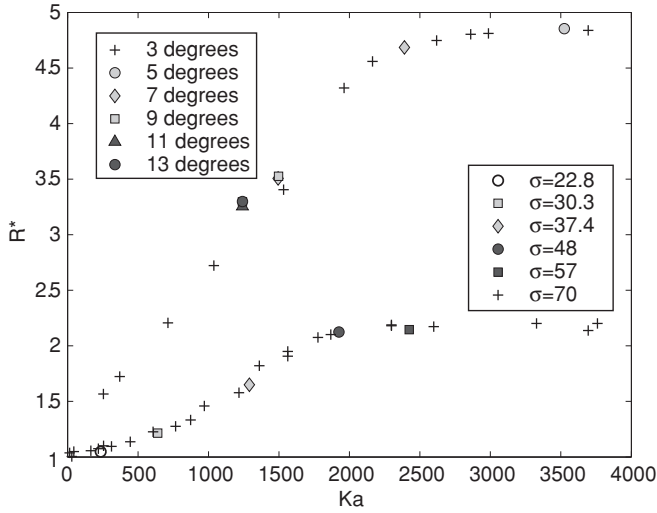


FIG. 1.  $R^*$  as a function of  $Ka$  for several angles, fluids, and widths. Surface tension is in mN/m. See text for details.

to kinematic viscosity, and (ii) the Kapitza number, defined as  $Ka = \sigma / (\rho g^{1/3} \nu^{4/3})$ , and representing the ratio of capillary to viscous stresses when the intrinsic viscous length and time scales,  $l_v = (\nu^2/g)^{1/3}$  and  $t_v = (\nu/g^2)^{1/3}$ , respectively, are used.  $\sigma$ ,  $\rho$ ,  $\nu$ , and  $g$  are, respectively, the surface tension, density, kinematic viscosity of the fluid, and the gravitational acceleration. Using the capillary length  $l_c = (\sigma/\rho g)^{1/2}$ , the Kapitza number is also  $Ka = (l_c/l_v)^2$ . The critical Reynolds  $Re_c$  for the primary instability was detected by local film thickness measurements with conductance probes, according to the method described in [17]. Spatial characteristics of traveling waves were documented by fluorescence imaging, as described in [18].

We revisit the previously observed [17] strong increase in  $Re_c$  for narrow channels and investigate systematically the dependence of the delay  $R^* = Re_c/Re_c^0$  on the physical properties of the liquid. A key result presently reported is that  $R^*$  correlates very satisfactorily only with the Kapitza number or the capillary number ( $Ca$ ), and not with other dimensionless parameters that are frequently used to express the effect of surface tension, such as the Weber ( $We$ ) or the Bond ( $Bo$ ) numbers. We recall that both  $Ka$  and  $Ca$  compare capillary to viscous forces, whereas  $We$  and  $Bo$  compare capillary to inertia and gravity forces, respectively.

We plot the results using  $Ka$  because it depends only on physical and not on flow properties. Data are shown in Fig. 1 for two channel widths and for a very wide range of  $Ka$ . The lower curve corresponds to  $W = 250$  mm and variation of  $Ka$  accomplished by changing either the viscosity or the surface tension. We observe that the choice is immaterial, and all data fall on the same curve. The upper curve corresponds to  $W = 100$  mm and data for channel inclinations in the range  $\theta = 3$ – $13^\circ$ . It is concluded that the delay  $R^*$  does not vary with inclination, at least in the range tested.

The functional dependence of the data in Fig. 1 indicates that the experimentally observed transition tends to the theoretical 2D prediction only in the limit of  $Ka \rightarrow 0$ . The deviation grows significantly with increasing  $Ka$ , and eventually reaches a plateau for  $Ka > 2500$ . With respect to this behavior, it is

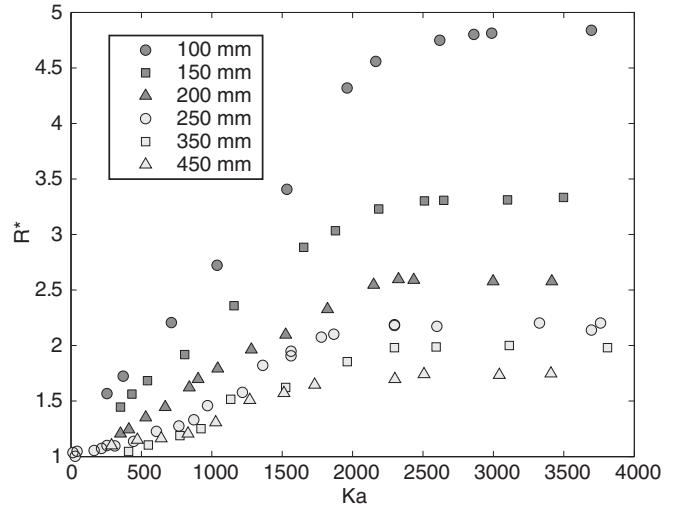


FIG. 2.  $R^*$  as a function of  $Ka$  for several widths  $W$ ,  $\theta = 3^\circ$ .

interesting to note that increasing the liquid viscosity causes a decrease in  $Ka$  and consequently results in lower critical  $Re$ , i.e., the flow is destabilized. As this is counterintuitive with the notion of viscous dissipation, it is conjectured that an additional attenuation mechanism is active at high  $Ka$ , when capillary forces dominate over viscous forces. This mechanism should fade out with decreasing  $Ka$ , thus permitting the flow to destabilize at lower  $Re$ .

Systematic investigation of the effect of channel width is undertaken in the range  $100 < W < 450$  mm, and the results are shown in Fig. 2. As expected, the wider the channel, the smaller the deviation from theory. However, differences are still very significant (i.e., exceed 60%) for the widest channel tested. Even more impressive, the deviation at high  $Ka$  for the 100 mm channel approaches 400%, although the ratio of width to film thickness is still deceptively high ( $> 100$ ). In the high  $Ka$  limit, the plateau values depend only on  $W$ , and are correlated satisfactorily by the hyperbolic fit  $R^* = 1 + 125/W^*$ , where  $W^* = W/l_c$ .

The aforementioned observations on the delay of the primary instability hint that when capillary forces dominate over viscous forces, there exists a strong transverse effect that bypasses the 2D dynamics and provides an inherently 3D capillary attenuation mechanism of the traveling disturbances. The onset of this effect may only be traced to the damping of free surface oscillations close to sidewalls, which is caused by (i) the thin viscous boundary layers and (ii) the resistance to the depinning of the contact line. In order to identify this capillary mechanism, we now focus on the characteristics of the waves that develop beyond the instability threshold.

Wave properties are documented by analyzing pictures taken with fluorescence imaging, which have been properly calibrated so that brightness is proportional to liquid film height. It was previously noted [18] that the first fully developed waves are not two dimensional, but acquire a parabolic crestline shape whose curvature depends on channel width. It is presently confirmed that this behavior depends strongly on  $Ka$ . More specifically, Fig. 3 shows snapshots of waves, in the 450 mm wide channel, created by regular inlet disturbances of frequency 2 Hz at roughly constant  $Re$ . With

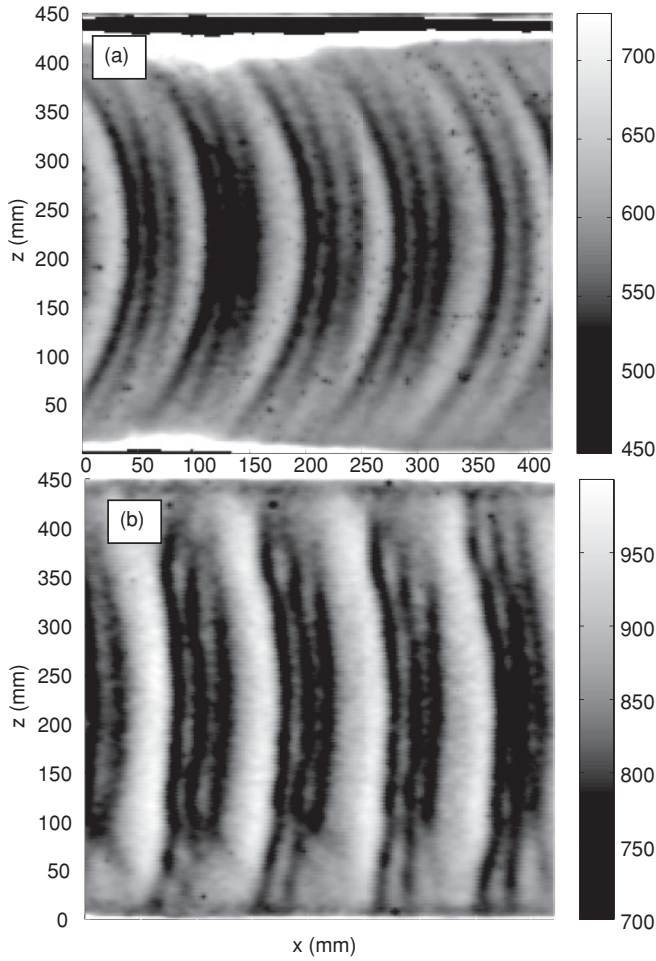


FIG. 3. Maps of the height  $h(x,z)$  for (a)  $Ka = 3100$  and (b)  $Ka = 1320$  at  $Re = 30$ ,  $f = 2$  hz,  $W = 450$  mm, and  $\theta = 3^\circ$ . The color bars indicate the height in microns.

decreasing  $Ka$ , the crestlines evidently become less curved, which is an indication that the 2D limit is approached.

It was argued above that oscillations close enough to the sidewalls should be damped by viscous and depinning resistance. If this is true, then the height of traveling waves should vary across the channel. These arguments are indeed supported by the data. In particular, Fig. 4 shows the variation in wave height moving along the curved crestline for three different values of  $Ka$ . The height is scaled by the Nusselt film thickness  $h_N$ , i.e., the thickness of steady film flow with undisturbed free surface at the same  $Re$ . Waves always attain maximum height at the channel center and decline toward the sides. However, the nonuniformity along the crestline, which can be taken as an indicator of deviation from 2D dynamics, increases with  $Ka$ . The dashed lines are mere tentative extrapolations, based on the conjecture that the liquid thickness close enough to the sidewalls is the Nusselt value [18].

The complete free surface structure of the aforementioned parabolic waves is presented in Fig. 5, corresponding to  $Re = 33$ ,  $f = 1$  hz,  $W = 450$  mm, and  $\theta = 3^\circ$ . It is readily noted that not only is the wave height at maximum at the center of the channel, but also a wide central region of minimum

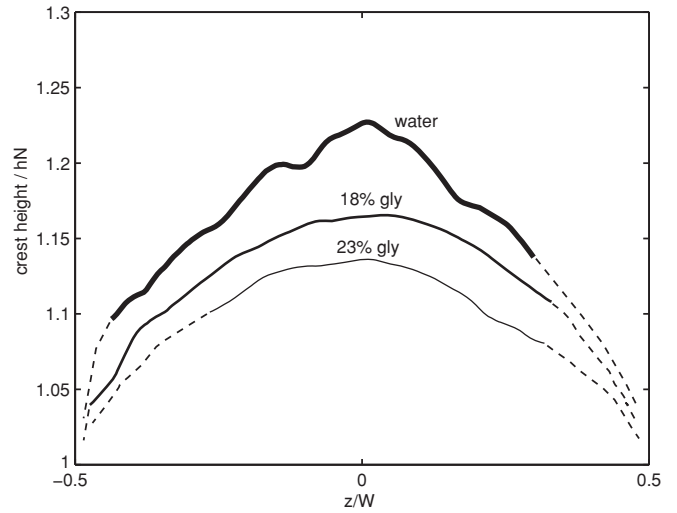


FIG. 4. Height of the crestline, normalized by corresponding Nusselt height, over the transverse direction for  $Ka = 3100$  (water), 1640 (18% glycerol), and 1320 (23% glycerol), at  $Re \approx 30$ ,  $f = 1$  hz,  $W = 450$  mm, and  $\theta = 3^\circ$ . Dashed lines are empirical extrapolations toward the walls.

film thickness forms behind this maximum. Thus, these high  $Ka$  waves have shape qualitatively similar to the lambda (or horseshoe) waves that are observed at much higher flow rates or inclinations [21,22], and are typical of genuinely three-dimensional dynamics.

The observed variation in film thickness results in a nonuniform pressure distribution inside the liquid. This distribution may drive secondary flows, particularly in the transverse direction where pressure differences are not balanced to leading order by other forces. We note also that the maximum wave height observed along the crestline at the channel center is reinforced by a local maximum of curvature below the main hump. The combined effect of hydrostatic and capillary

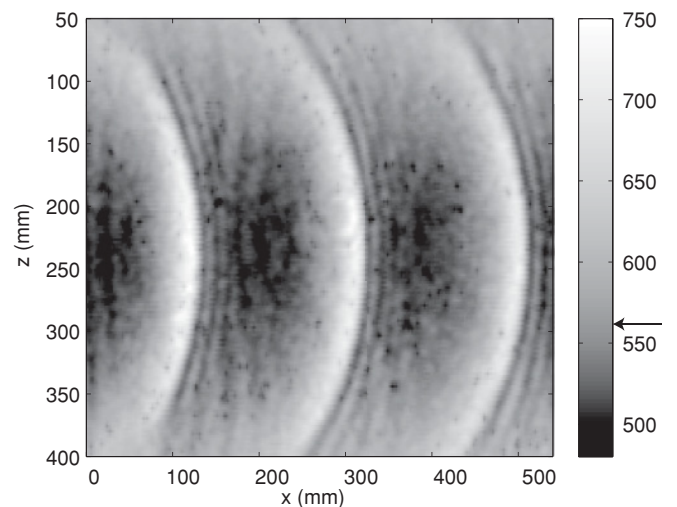


FIG. 5. Map of the height  $h(x,z)$  at  $Re = 33$ ,  $f = 1$  hz,  $W = 450$  mm, and  $\theta = 3^\circ$ . The color bar indicates the height in microns and the arrow indicates the Nusselt height.

pressure below the hump should direct liquid from the center toward the sides along the crestline. On the contrary, the variation in substrate thickness, from a value close to  $h_N$  at the sides toward the minimum at the center, should drive liquid in the opposite direction. Thus, a secondary flow consisting of two closed eddies, symmetric with respect to the channel centerplane, should be established.

The above conjectured secondary flow provides an additional (transverse) draining mechanism for the traveling disturbances. This mechanism is evidently more efficient in narrow channels and for liquids with high surface tension. For example, in the case depicted in Fig. 5, the hydrostatic pressure gradient in the transverse direction is estimated as  $\Delta P_h \sim \rho g(h - h_N)/2 \sim 1$  Pa, and the capillary pressure gradient in the transverse direction is estimated as  $\Delta P_c \sim |\sigma d^2 h/dx^2| \sim 0.5$  Pa. Thus, in the high  $Ka$  limit, capillary forces become comparable to hydrostatic forces in their potential to drive a secondary flow. It is recalled that the 2D mechanism for arresting solitary wave growth is capillary dissipation, i.e., the enhanced streamwise, viscous dissipation at the small scales introduced by capillary deformation. It is presently argued that at high enough values of  $Ka$ , the transverse draining mechanism prevails over streamwise dissipation, and thus postpones the appearance of the primary instability to higher  $Re$ .

Numerical simulations could serve to confirm the above-conjectured draining mechanism for traveling disturbances. As a 3D simulation of the complete Navier-Stokes equations with a deformable free surface still represents a formidable task, reduced versions based on long-wave expansions could be used [7]. The present data (Fig. 4) indicate that an effective

boundary condition in the transverse direction could combine no penetration and zero wave height.

### III. CONCLUSIONS

To conclude, we have presented experimental evidence that the delay in the primary instability of inclined film flows in channels of finite width scales with the ratio of capillary to viscous forces, as expressed by the Kapitza number. The deviation from the theoretical 2D prediction increases with  $Ka$ , and reaches a plateau for high enough values. This behavior testifies to a bypass of the 2D evolution stage of the instability due to an inherently 3D wave attenuation mechanism, which apparently stems from the effect of the sidewalls. The dependence of the phenomenon on channel width, in combination with the strength of the deviation for large  $W/h_N$  ratios, indicates the existence of long-range transverse coherence in this typical example of an active dispersive-dissipative nonlinear medium. Examination of the first post-threshold traveling waves supports the notion that the long-range coherence is provided by a draining mechanism of the disturbances, which is related to the transverse nonuniformity in the wave characteristics.

### ACKNOWLEDGMENTS

The present work was supported by the EU under the Marie-Curie Initial Training Network ‘‘Multiflow’’ (GA No. 214919-2) and by Program ‘‘Hrakleitos II’’ of the Greek Ministry of Education.

- 
- [1] A. Oron, S. H. Davis, and S. G. Bankoff, *Rev. Mod. Phys.* **69**, 931 (1997).
  - [2] H. C. Chang and E. A. Demekhin, *Complex Wave Dynamics on Thin Films* (Elsevier, Amsterdam, 2002).
  - [3] R. V. Craster and O. K. Matar, *Rev. Mod. Phys.* **81**, 1131 (2009).
  - [4] M. G. Velarde and A. A. Nepomnyashchy, *Solitons in Viscous Flows*, Lect. Notes Phys., Vol. 751 (2008), p. 1–21.
  - [5] H. C. Chang, *Annu. Rev. Fluid Mech.* **26**, 103 (1994).
  - [6] S. Saprykin, E. A. Demekhin, and S. Kalliadasis, *Phys. Rev. Lett.* **94**, 224101 (2005).
  - [7] B. Scheid, C. Ruyer-Quil, and P. Manneville, *J. Fluid Mech.* **562**, 183 (2006).
  - [8] J. Liu and J. P. Gollub, *Phys. Rev. Lett.* **70**, 2289 (1993).
  - [9] H. C. Chang, E. A. Demekhin, and E. N. Kalaidin, *J. Fluid Mech.* **294**, 123 (1995).
  - [10] H. C. Chang, M. Cheng, E. A. Demekhin, and D. I. Kopelevich, *J. Fluid Mech.* **270**, 251 (1994).
  - [11] J. Liu, J. B. Schneider, and P. J. Gollub, *Phys. Fluids* **7**, 55 (1995).
  - [12] C. D. Park and T. Nosoko, *AIChE J.* **49**, 2715 (2003).
  - [13] E. A. Demekhin, E. N. Kalaidin, S. Kalliadasis, and S. Y. Vlaskin, *Phys. Fluids* **19**, 114103 (2007).
  - [14] J. Liu, J. D. Paul, and J. P. Gollub, *J. Fluid Mech.* **250**, 69 (1993).
  - [15] J. Liu and J. P. Gollub, *Phys. Fluids* **6**, 1702 (1994).
  - [16] S. V. Alekseenko, V. E. Nakoryakov, and B. G. Pokusaev, *Wave Flow of Liquid Films* (Begell, New York, 1994).
  - [17] M. Vlachogiannis, A. Samandas, V. Leontidis, and V. Bontozoglou, *Phys. Fluids* **22**, 012106 (2010).
  - [18] V. Leontidis, J. Vatteville, M. Vlachogiannis, N. Andritsos, and V. Bontozoglou, *Phys. Fluids* **22**, 112106 (2010).
  - [19] T. B. Benjamin, *J. Fluid Mech.* **2**, 554 (1957).
  - [20] M. Scholle and N. Aksel, *ZAMP* **52**, 749 (2001).
  - [21] S. V. Alekseenko, V. A. Antipin, V. v. Guzanov, S. M. Kharlamov, and D. M. Markovich, *Phys. Fluids* **17**, 121704 (2005).
  - [22] E. A. Demekhin, E. N. Kalaidin, S. Kalliadasis, and S. Y. Vlaskin, *Phys. Fluids* **19**, 114104 (2007).